

# Stability of Self-Assembled Hydrophobic Surfactant Layers in Water

Susan Perkin,<sup>†</sup> Nir Kampf,<sup>§</sup> and Jacob Klein<sup>\*,†,§</sup>

Physical and Theoretical Chemistry Laboratory, South Parks Road, Oxford, OX1 3QZ, United Kingdom, and Weizmann Institute of Science, Rehovot 76100, Israel

Received: May 25, 2004; In Final Form: November 30, 2004

Using contact angle measurements, surface force balance experiments, and AFM imaging, we have investigated the process of self-assembly of surfactants onto mica and the subsequent stability of those layers in pure water. In the case of cetyltrimethylammonium bromide (CTAB), the stability of a monolayer when immersed in pure water is found to be dependent on initial immersion time in surfactant, which is likely to be caused by an increase in the proportion of ion-exchange to ion-pair adsorption when incubated in surfactant for longer periods of time. Infinite dilution of the surfactant solution before withdrawal of the sample is found to have little effect on the stability of the resulting layer in pure water. The nature of the counterion is found to affect dramatically the stability of a self-assembled surfactant monolayer: cetyltrimethylammonium fluoride (CTAF) forms a layer that is much more stable in water than CTAB, which is likely to be due to faster and more complete ion-exchange with the mica surface for CTAF. Surface force balance experiments show that when the hydrophobic monolayer is immersed in pure water it does not simply dissolve into the water; instead it rearranges, possibly to patches of bilayer or hemimicelles. The time scale of this rearrangement agrees well with the time scale of the change from a hydrophobic to more hydrophilic surface observed using contact angle measurements. AFM imaging has also in some cases shown an evolution from an even monolayer to patches of bilayer.

## Introduction

The self-assembly of surfactant molecules into arrays with long range order both in solution and at surfaces gives them a uniquely important role in industrial and household applications as well as in naturally occurring biological systems.<sup>1–3</sup> The nature of the self-assembly process in solution<sup>3</sup> and at the surface<sup>3–6</sup> and of the aggregates formed<sup>7–12</sup> are matters of interest. The interactions between surfactant layers across aqueous media, both in the normal and shear directions, are particularly important: Investigation of the hydrophobic interaction<sup>13–16</sup> suggests the importance of hydrophobic patches in protein folding, and measurements of shear stress between di-chain cationic surfactants [W. Briscoe et al., in preparation] give clues to the importance of charged headgroups in biological lubrication.

Many of these experiments have been carried out using the surface force balance (SFB), with mica as a substrate for the surfactant molecules. In the case of less water soluble surfactants the molecules are often deposited onto the mica by a Langmuir–Blodgett method,<sup>17,18</sup> whereas water soluble surfactants tend to be self-assembled onto the surfaces from solution<sup>4,13,15</sup> in which case the experiment is carried out inside the surfactant solution. However, in some cases it is desirable to have a surfactant monolayer that is stable in pure water, for example when using the hydrophobic surface as a substrate for adsorbing macromolecules,<sup>19</sup> or when one surface is hydrophobic and the other hydrophilic.<sup>20</sup> It is the aim of this work to investigate the stability of a hydrophobic surfactant layer, adsorbed by self-assembly onto mica, when submerged in pure water.

When a cationic surfactant adsorbs to a negatively charged surface such as mica, the molecules can be bound in 2 ways: “Ion-exchange” with the surface can occur, whereby the counterion is dissociated into solution and the remaining positively charged surfactant molecule attaches to a negative site on the mica (charge–charge, or Coulombic, interaction). Alternatively, the un-dissociated surfactant molecule can bind to the mica as an ion pair (charge–dipole interaction). The latter is likely to be a weaker bond than the former, with a lower energy barrier to desorption, and therefore will lead to a less stable hydrophobic layer. XPS measurements have shown that during self-assembly ion pairs initially adsorb, then the counterion subsequently dissociates to leave Coulombically bound headgroups at the surface.<sup>4</sup> This result coincides well with observations that Langmuir–Blodgett deposition of the surfactant in some cases does not result in a hydrophobic layer stable in water.<sup>21</sup> The effect of the counterion on the self-organization structures of ionic surfactants in the bulk solution has been investigated.<sup>22–25</sup> Different counterions have very different solvation properties in water, and the hydration of counterions influences directly the binding of the ion to the aggregate surface. This difference in counterion binding in turn changes the inter- and intraaggregate electrostatic interactions. Thus exchanging the counterion induces significant changes in the general phase equilibria and in the sequence of aggregates formed at varying concentrations and temperatures.<sup>26</sup> The effects of altering the counterion on surface structures and monolayer packing have been studied at the liquid–air interface,<sup>27</sup> as have the effects on the adsorption kinetics at the solid–liquid interface,<sup>4</sup> and the interactions between monolayers and bilayers of surfactant.<sup>28,29</sup>

How can we alter the self-assembly procedure to maximize the stability of the hydrophobic layer in water? In this study

\* Author to whom correspondence should be addressed. E-mail: jacob.klein@chem.ox.ac.uk.

<sup>†</sup> Physical and Theoretical Chemistry Laboratory.

<sup>§</sup> Weizmann Institute of Science.

the effect of altering the self-assembly immersion time is reported, and discussed in the context of the ratio ion-exchange to ion-pair adsorption. We also report a remarkable difference in the stability of a hydrophobic layer when the surfactant counterion is changed from bromide to fluoride. The hydrophobicity of the resulting layers is recorded using contact angle measurements; the topography of the layer under water is monitored with AFM; and the interactions between two hydrophobised surfaces in water are examined using the surface force balance.

## Materials

Cetyltrimethylammonium bromide ( $\text{CH}_3(\text{CH}_2)_{15}\text{N}(\text{Me})_3\cdot\text{Br}$ ), CTAB, was Fluka puriss p.a., and didodecyltrimethylammonium bromide ( $((\text{CH}_3(\text{CH}_2)_{11})_2\text{N}(\text{Me})_2\cdot\text{Br})$ , DDAB, was Fluka purum grade, both used as received. Cetyltrimethylammonium fluoride ( $\text{CH}_3(\text{CH}_2)_{15}\text{N}(\text{Me})_3\cdot\text{F}$ ), CTAF, kindly donated by Dr. C. Bain, was synthesized from the hydroxide using an ion-exchange resin together with HF, and then re-crystallized from acetone with a trace of methanol.<sup>27</sup> Gemini-12 surfactant ( $((\text{C}_{12}\text{H}_{25})(\text{N}(\text{Me})_2)(\text{C}_6\text{H}_{12})(\text{N}(\text{Me})_2)(\text{C}_{12}\text{H}_{25})\cdot\text{Br}_2)$ ) was synthesized by Dr. Z. X. Li and Dr. R. K. Thomas according to the method of Menger and Littau.<sup>30</sup> Pure conductivity water was obtained by treating tap water with activated charcoal followed by a Millipore water purification system, consisting of RiOs and MILLI-Q Gradient (A10) stage. The total organic content was 3–4 ppb and resistivity >18.2 M $\Omega$ .

## Methods

**Preparation of Surfactant-Coated Mica Surfaces by Self-Assembly.** Mica sheets of approximately 1 cm  $\times$  2 cm  $\times$  0.1 mm were cleaved on both sides immediately prior to use. They were then immersed in surfactant solution above the CMC (0.1% w/w for CTAB, approximately 3 times the CMC) for a fixed time before withdrawing at a rate of  $1.0 \pm 0.5$  mm/s. The mica appeared “wet” at this stage, presumably due to adsorbed micelles and bilayers creating a hydrophilic surface. It was then rinsed by dipping in 25 mL of pure water for 20 s to remove these outer un-bonded molecules. The resulting surface appeared completely dry and was clearly hydrophobic. The mica sheets were then placed in beakers of pure water, and after time  $t$  ( $t = 0$ –1500 min) were removed and left to dry for 5–10 min before contact angle or AFM measurements were performed. The mica sheets were never re-immersed in water; a completely new piece was used for each single measurement. The whole preparation process was carried out in a laminar flow cabinet to avoid particulate contamination.

In some experiments an “infinite dilution” technique was used in order to eliminate the stage of removing the mica through the surfactant solution–air interface. In these cases the 15 mL solution was rinsed through with >5 L of pure water before withdrawal of the mica.

**Contact Angle Measurements.** Advancing contact angles of pure water were measured on mica sheets after coating in surfactant as described above, using a Ramé-Hart Inc. Goniometer and imaging software RHI2001. The measurements were made in a sealed and humidified chamber at the ambient temperature of 28  $^\circ\text{C}$ , and care was taken to level the sample. Droplets of pure water were placed on the substrate, and water was added at a constant rate while taking the measurement of the advancing contact angle. The drop volumes were typically  $1.5 \pm 0.5$   $\mu\text{L}$ . The scatter in these measurements was found to be  $<1^\circ$  for a given surface, although variations of up to  $10^\circ$

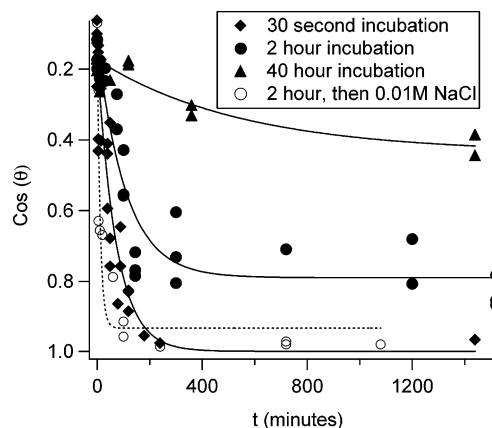


**Figure 1.** Advancing contact angles of pure water on self-assembled CTAB layers on mica, after soaking the layer in water (or 0.01 M NaCl, open circles) for time  $t$ . Three different initial incubation times in surfactant solution are represented: 30 s ( $\blacklozenge$ ), 2 h ( $\bullet$ ,  $\circ$ ), and 40 h ( $\blacktriangle$ ). The initial contact angle (without soaking in water at all) is very similar in each case,  $82 \pm 5^\circ$ ; however, the decay rate as the mica sheets are soaked in water decreases and the final “equilibrium” angle after large times in water increases with increasing self-assembly time. For the 2 h incubation time, we compare incubation in pure water ( $\bullet$ ) and 0.01 M NaCl solution ( $\circ$ ). We emphasize that mica sheets were never re-immersed in water; each data point corresponds to an entirely new mica sheet.

were observed between entirely separate mica sheets and surfactant solutions when the same preparation procedure was followed.

**SFB Measurements.** The SFB technique has been described earlier.<sup>31–33</sup> Mica was cleaved to molecularly smooth (single facet) sheets of thickness 1–2  $\mu\text{m}$ . These were laid onto a freshly cleaved backing sheet, silvered, glued onto cylindrical glass lenses, and mounted inside the apparatus. After calibrating the system in air, pure water was added and the normal and shear forces between the mica surfaces were measured. It has been found to be imperative to conduct this pure water stage in all aqueous experiments; only when the long-ranged osmotic repulsion is followed by a jump-in to adhesive contact, and the shear measurements reveal no detectable lateral forces until after this jump, is the system considered clean. Any experiment that shows a repulsive force of longer range or higher force than expected or does not exhibit the van der Waals jump-in to contact is discarded. After calibration in water the lenses were removed from the apparatus and incubated in  $1 \times 10^{-3}$  M CTAB solution for 2 h, rinsed in pure water for 20 s, and replaced inside the apparatus in pure water. Normal forces were measured as a function of separation distance and as a function of time after the surfactant coated mica surfaces were placed in the pure water.

**AFM Imaging.** AFM imaging was with a Nanoscope III instrument in both contact and tapping mode. Samples were prepared as described above then mounted inside the microscope with a large droplet of water on top. The fluid cell was then placed above the droplet with the cantilever inside, where imaging took place. Images were recorded as a function of time after adding water to the sample.

## Results and Discussion

**(a) Contact Angle Measurements.** In Figure 1 the diamond symbols ( $\blacklozenge$ ) show a typical series of contact angle measurements on mica sheets prepared by dipping into 0.1% w/w CTAB solution for 30 s then (after rinsing) into pure water for varying times,  $t$ . For CTAB coated mica sheets not soaked

in water at all other than the 20 s rinse ( $t = 0$ ), the initial contact angle of water on the monolayer is  $82 \pm 5^\circ$ . As the incubation time of the layer in water increases, the subsequent advancing contact angle decreases. Mica sheets incubated in water for  $>200$  min have reached equilibrium, and have contact angles of  $15 \pm 10^\circ$ .

The hydrophilisation of the surface during incubation in water could be explained a number of ways: The simplest explanation is that individual molecules are desorbing from the monolayer into solution, gradually revealing the hydrophilic mica surface. Alternatively, the layer could be gradually undergoing a rearrangement. This rearrangement could involve the overturning of individual molecules in the layer from a position of hydrophobic tail outermost to one of charged headgroup outermost, or could involve overturning of whole patches of the layer. In all of these cases charged headgroups must detach from the mica surface, and the energy required for this to occur will depend on the nature of the binding: ion-exchange or ion-pair adsorption. (The decrease in hydrophobicity after immersion in water has been observed in the past<sup>6</sup> using the “ageing droplet” technique; however, the situation is complicated in that case by the effects of the 3 phase line at the edge of the droplet.)

Also shown in Figure 1 are data for mica surfaces incubated in CTAB solution for longer periods of time (●, 2 h; ▲, 40 h). The initial contact angle ( $82 \pm 5^\circ$ ) is similar in each case. However, the rate of decay in contact angle for mica sheets immersed in pure water as well as the equilibrium contact angle reached after long times is dependent on the incubation time in surfactant. This is likely to be due to the degree of ion-exchange on the mica surface: For the 30 s adsorption the molecules are mainly bound by ion-pair-charge attraction (as opposed to charge-charge attraction) because there has been insufficient time for the counterions to desorb and work their way through the hydrophobic region of surfactant tails during the incubation period. Thus after sufficiently long periods of time in pure water these mostly (weak) ion-pair bound surfactants have “doubled up” (see later), exposing hydrophilic mica and hydrophilic bilayers, and the surface becomes almost entirely hydrophilic. In contrast a 40 h adsorption achieves a larger degree of ion-exchange with the mica surface during the longer incubation period, leading to a layer much more of which is bound by the stronger charge-charge attractions, and which is therefore less easily displaced in pure water, and remains significantly hydrophobic after long periods of time in water. For the 2 h incubation time, we compare results for incubation in pure water (solid circles) and in 0.01 M NaCl solution (open circles). The decay in hydrophobicity is much more rapid in salt solution, and continues toward a more hydrophilic equilibrium state. In addition to the charge/dipole effects, the adsorption density could be affected by incubation time in surfactant and thus contribute to some extent to the observed differences in stability: XPS measurements have shown<sup>4</sup> that for a similar system the adsorption density increases by  $\sim 15\%$  between 30 s and 2 h of incubation in solution.

We do not expect the structure of the surfactant during these contact angle experiments to be as it was inside the water bath as it has been removed and dried. Removing the sample from the water is likely to cause the outer layer of surfactant bilayer raft (see later) or any un-bound molecules to be removed, and remaining molecules to be re-distributed. (The remaining molecules may well lie flat on the surface.) There was some hysteresis between advancing and receding contact angles on these samples, suggesting that the surface was not entirely heterogeneous. (This may be dependent on the drying time of

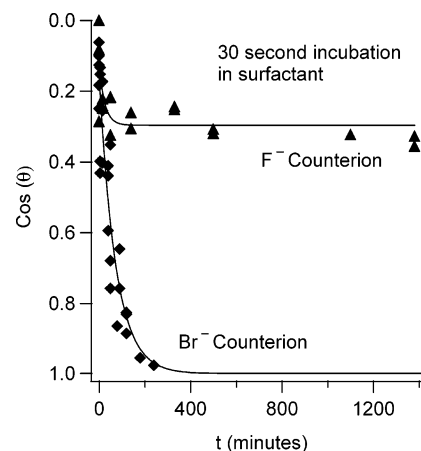


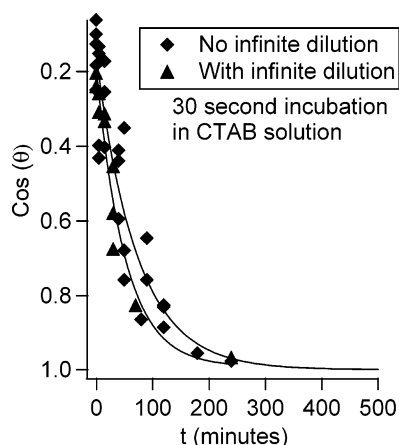
**Figure 2.** The effect of changing the headgroup from bromide (CTAB, diamonds) to fluoride (CTAF, triangles). The solutions used to incubate the mica were just above the respective surfactant CMCs: 0.1% w/w for CTAB and 0.2% w/w for CTAF.

the sample, and this parameter was not studied.) AFM studies of the dried CTAB layer on withdrawal following extended incubation in the water indicate that the molecules appear in some cases to be uniformly spread over the surface, and in other cases remain in patches.

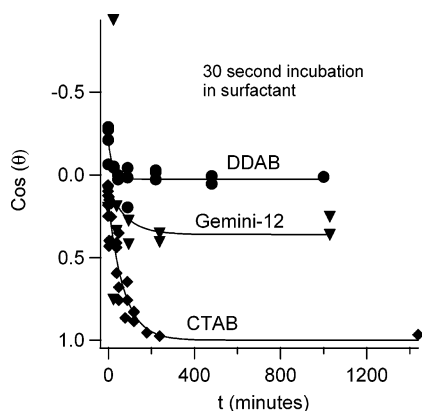
If the stability of the adsorbed monolayer of surfactant on mica is indeed dependent on the degree of ion-exchange, then the nature of the counterion is likely to be important. In Figure 2 we present a comparison of the stability in pure water of two surfactant monolayers: CTAB and CTAF. The equilibrium contact angle of water on the CTAF layer after long immersion in pure water is  $70 \pm 2^\circ$  in comparison to  $15 \pm 5^\circ$  for CTAB. The surfactant molecules seem to remain to a large extent bound to the surface exposing hydrophobic tails when adsorbed from CTAF even when exposed to water for long periods of time, while the layer adsorbed from CTAB solution does not. We attribute the reason for this difference between CTAB and CTAF as follows: In the case of the CTAF solutions, a much larger proportion of the surfactant molecules have dissociated due to the greater propensity for hydration of the fluoride (compared to the bromide) ion. Thus the fraction of the surfactant surface layer initially bound by charge-charge interaction is much higher, and moreover, with longer incubation time, further ionization of any ion-pair bound molecules occurs more readily than for the bromide layers. The overall effect therefore is that, for a given incubation time, the CTAF layers are more stably bound and so are more resistant to desorption (and its consequent hydrophilisation effect) when immersed in pure water.

To separate the effects of solution adsorption and adsorption at the 3 phase line during withdrawal from surfactant solution, an experiment was carried out in which the CTAB solution was “infinitely diluted” before the mica was withdrawn so that when the mica eventually was removed through the meniscus there could not be deposition at the 3 phase line. The result of this experiment is shown in Figure 3, with comparison to the previous (nondilution) result (▲, infinite dilution; ◆, no dilution). It is clear that infinite dilution of the solution before withdrawal of the mica through the meniscus has little effect on the stability or decay in hydrophobicity in water of the layer formed, indicating that the ion-exchange process is independent of withdrawal effects. It is of course likely that some CTAB molecules do adsorb onto the surface at the 3 phase line when the solution is not infinitely diluted, on top of the layer formed inside the solution; however, it seems that the rinsing step washes off these weakly bound molecules.





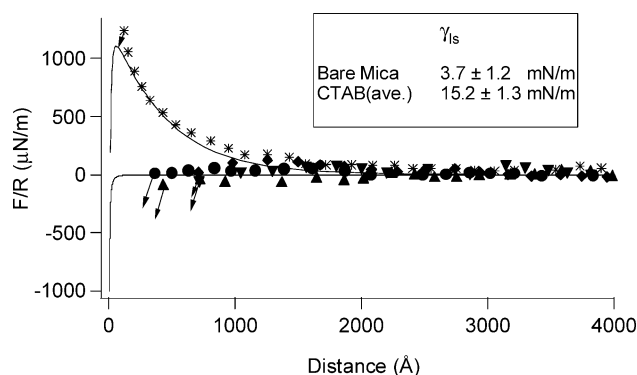
**Figure 3.** Comparison of the "ordinary" dipping procedure where the mica is withdrawn through the three-phase line after incubation in the solution (◆) with an infinite dilution method as described in the text (▲). Each data point corresponds to a new mica sheet, and each sheet was incubated in solution for 30 s before withdrawal or infinite dilution.



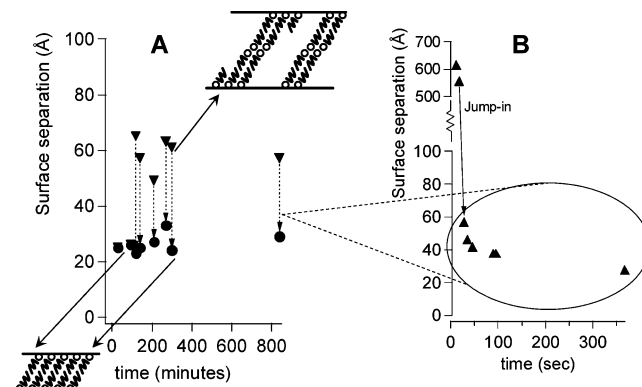
**Figure 4.** Advancing contact angles of pure water on self-assembled CTAB (◆, same data as in Figure 1), Gemini-12 (▲), and DDAB (●). In each case the immersion time in surfactant was 30 s.

Figure 4 compares the results for CTAB stability after a 30 s adsorption time to similarly prepared layers of DDAB and Gemini-12 surfactants. In each case there is some hydrophilisation of the layer after soaking in pure water, but the equilibrium layers for Gemini-12 and DDAB surfactants are still very hydrophobic; ion exchange with the mica surface for these molecules appears to happen more quickly than for CTAB. In the case of the Gemini surfactant this may be because only one of the headgroups on each molecule need be ion-exchanged in order to make the whole molecule irreversibly bound.

**(b) Surface Force Balance Measurements.** Figure 5 shows normal force profiles between two bare mica surfaces in pure water and between self-assembled CTAB layers across pure water. Between bare mica in water the forces are well described by DLVO theory and have been discussed in detail elsewhere.<sup>34–36</sup> Once the mica surfaces have been coated with a layer of surfactant the forces between them (from large separations down to separations of approximately 300–500 Å) remain close to zero (for the first approach at each contact position), suggesting that the presence of the surfactant neutralizes the surface charge. From a distance of 300–500 Å the surfaces spontaneously jump into contact, and this behavior is not significantly altered over the period of time of the experiment. The long range of this jump-in cannot be explained purely as a van der Waals interaction, which is indicated by the solid line. This behavior is characteristic of that between two hydrophobic surfaces interacting across a polar medium<sup>13,14,16,35,37</sup> although its origin



**Figure 5.** Normal force profiles measured using the surface force balance. Interactions between bare mica across conductivity water (stars) show an osmotic repulsive force due to the overlap of the electrical double layers, followed by a jump-in to adhesive contact (arrow). This interaction is well described by a linearized DLVO expression:<sup>3</sup>  $F/2\pi R = 64Ck_B T \kappa^{-1} \tanh^2(e\Psi/4k_B T) \exp(-\kappa D) - A/12\pi D^2$ , where  $C$  = electrolyte concentration,  $T$  = temperature,  $k_B$  = Boltzmann constant,  $A$  is the Hamaker constant of mica across water ( $2 \times 10^{-20}$  J),  $\Psi$  is the effective surface potential, and  $\kappa^{-1}$  is the Debye length. From this fit to our data we obtain  $C = 5.5 \times 10^{-5}$  M and  $\Psi = 100$  mV. The interactions between the same mica surfaces once a CTAB layer has been self-assembled onto them are shown by the filled symbols. Four separate compression force profiles are shown; each is from a different contact position on the mica surface, each is measured after a time >100 min following immersion in the water-filled bath (up to times of 17 h), and each is the first approach at that contact position. The arrows indicate the point after which a jump-in to adhesive contact was observed. The inset table gives the liquid–solid surface energy  $\gamma_{ls}$  values, calculated as described in the text.



**Figure 6.** (A) The separation of the surfaces (relative to bare mica contact) after the jump-in is shown, as a function of time relative to  $t = 0$  when the surfaces were coated in CTAB and immersed in conductivity water. The triangular markers indicate the position immediately after the jump. The surfaces then spontaneously squeeze closer together (over a few minutes; see part B), as shown by the dashed arrows, until they reach their final separation shown by the circular markers. The first two markers, in the region below 100 min, show that during this period the surfaces jumped immediately to the separation of  $25 \pm 3$  Å and did not move from this separation. The inset diagrams represent a possible explanation for the effect: Surfaces jump to partial bilayer–bilayer contact then squeeze closer until they reach monolayer–monolayer contact. (B) A more detailed picture of one of the "squeeze together" effects shown in part A. (Notice that the time scale in part B is seconds compared to minutes for part A; the section circled in part B is an expansion of one of the profiles in part A.) This time the jump-in is indicated by the solid arrow, and the subsequent data points after the jump show the surfaces coming closer together while continually in flattened contact. The time scale is relative to an arbitrary zero somewhere just before the jump.

has not so far been entirely resolved. It has been suggested that this effect may be caused by air bubbles adsorbed at the hydrophobic–hydrophilic interface.<sup>38,39</sup> After jumping into

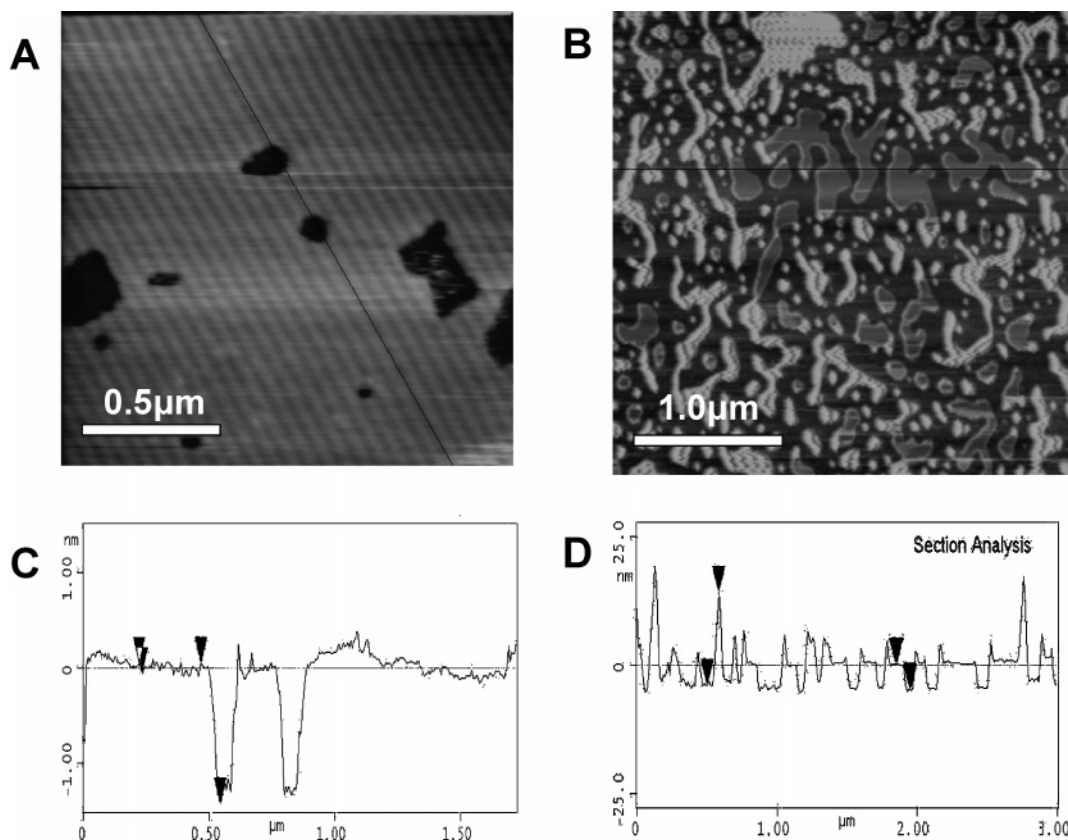


**Figure 7.** (A) AFM image of the CTAB layer recorded 5 min after addition of water to the surface. The dark areas are holes in the surfactant monolayer. The regular diagonal lines are electronic noise. (B) A cross-section trace at the black line in image A. The depth of one of the holes is  $14 \pm 3$  Å and the rms roughness is 2 Å. (C) Tapping mode image after 20 min under conductivity water at the same position on the surface as in part A; a rearrangement in the CTAB layer is observed. This rearrangement was not due to the act of scanning the surface; other areas also showed the same pattern when the probe was moved directly to them (i.e. it did not require 20 min at each contact position). Islands of surfactant, of two distinct heights (shades), are surrounded by areas of regular height, which is likely to be bare mica. Image analysis reveals that very close to half of the total area is taken up by the bare mica. Due to conservation of volume of surfactant from the original monolayer, the remaining islands of surfactant can be no higher than bilayer; they could be less if some is dissolved. (It is possible that the lightest areas are caused by the probe tip sticking to the surfactant and heightening the layer as it scans.)

contact the surfaces adhere to one another, and pull apart only when the deflection of the spring reaches a point  $\delta$  where

$$\delta = F_{\text{adh}}/k$$

for spring constant  $k$ . Thus the adhesive force  $F_{\text{adh}}$  can be calculated from the separation distance after the jump, which is equivalent to  $\delta$ . Using JKR theory<sup>40</sup> the interfacial energy,  $\gamma_{\text{sl}}$ , can now be calculated:

$$\gamma_{\text{sl}} = -F_{\text{adh}}/3\pi R$$

which gives us  $\gamma_{\text{sl}} = 3.7 \pm 1.2$  mN/m for bare mica in water (which is close to previously reported values<sup>41</sup>), and  $\gamma_{\text{sl}} = 15.2 \pm 1.3$  mN/m for CTAB coated mica across water. This behavior was only observed for the *first approach* at each contact position; on subsequent approaches long-range repulsive forces and instabilities were observed which we suggest are due to break up of the layer into surface-adsorbed aggregates (caused by the jump-out of contact from the first approach). We should note that the surfaces at the later times continue to jump-in from a large separation, despite the fact that, as seen in Figure 1, they are by no means entirely hydrophobic. [The long-ranged attraction between surfaces comprising patches of positive and negative charge (as we infer from the contact angle, SFB and AFM results in the next section) is not trivial to account for. It is possible that it originates as the charge patches shift across

the surface to a correlated orientation, with positive bilayer rafts opposite negative mica surface areas (S. Perkin, N. Kampf, J. Klein, submitted).]

Over the course of the experiment, the absolute separation of the mica surfaces immediately after the jump-in changed from  $25 \pm 2$  Å (corresponding to monolayer–monolayer contact) to  $57 \pm 8$  Å, as shown by triangles in Figure 6A. The time scale over which this change takes place is approximately 100 min after submerging the CTAB coated surfaces in water, which coincides with “hydrophilisation time” for a 2 h incubation in surfactant (Figure 1; recalling that the CTAB coated surfaces in the SFB were indeed incubated in surfactant solution for 2 h). This increase in contact separation immediately after the jump was reproducible between contact positions, and did not increase further for long periods of time (up to 14 h). In each case the absolute separation was then periodically recorded over the next few minutes after the jump-in. The separation decreased slowly, seeming to “squeeze out” some surfactant, until reaching a final separation of  $26 \pm 7$  Å (Figure 6A, dashed arrows and round markers). It appears that after 100 min the surfactant monolayers have rearranged into surface structures of double thickness  $\sim 57$  Å, possibly spherical or cylindrical aggregates<sup>42</sup> or patches of bilayer, which are compressible and therefore allow the surfaces to slowly squeeze closer until they reach the minimum separation corresponding once again to monolayer–

monolayer contact. A more detailed representation of the squeezing out of surfactant after the jump-in is given in Figure 6B.

**(c) AFM Imaging.** Figure 7 shows AFM images of a CTAB layer on mica under pure water. After 5 min in water (Figure 7A) the layer is very smooth (rms roughness  $<2$  Å) with some defects which are likely to be holes through to the mica. The thickness of the layer, using the holes as a baseline, is  $13 \pm 2$  Å (Figure 7B). This value is the same within error as half the observed thickness of two contacting layers measured inside the surface force balance. After 20 min in water, the layer rearranges to leave islands of surfactant surrounded by bare mica (Figure 7C). These islands are mostly twice the height of the original monolayer (and sometimes significantly higher), as shown in the cross section (Figure 7D). We suggest that the monolayer has rearranged to patches of bilayer with some larger aggregates. This behavior could well explain the SFB observations described above: the two surfaces initially come into bilayer–bilayer contact, which then compresses due to the incomplete bilayer coverage. (The time scale of this rearrangement is shorter than that observed in the SFB, probably because the incubation time of the mica in solution was also shorter.) This is also in agreement with the contact angle result: the hydrophilisation with time is due to the rearrangement of the hydrophobic monolayer into patches, or rafts, of headgroup-exposed bilayer (positively charged) surrounded by negatively charged mica.

## Conclusions

We have investigated aspects of the self-assembly of surfactants at the mica–solution interface, and the stability under pure water of the resulting layer. We conclude that for CTAB surfactant the incubation time of the surface in solution is crucial to the stability of the ensuing layer, with time scales for conservation of hydrophobicity under water in the region of tens of hours. The surfactant counterion is found to be very significant to the stability of the layer; other things being equal CTAF creates a much more stable and hydrophobic layer than CTAB. We attribute this counterion effect to the greater propensity of fluoride ions to hydrate, compared with the bromide ions, which in turn enhances the proportion of more stable charge–charge attachments of CTAF surfactants to the mica surface. SFB and AFM experiments together provide evidence for a rearrangement of the hydrophobic monolayer under water into aggregates and patches of bilayer, on time scales similar to the hydrophilisation observed in contact angle measurements.

**Acknowledgment.** We thank Dr. Wuge Briscoe, Dr. Colin Bain, Dr. Robert K. Thomas, and Ms. Liraz Chai for helpful discussions. We particularly thank Dr. Colin Bain for the CTAF surfactant, Dr. Robert K. Thomas, Dr. Z. X. Li, and Dr. Chu Chuan Dong for the Gemini-12 surfactant, and Dr. Sidney Cohen for the AFM imaging. We thank the EPSRC (UK) for a studentship (S.P.) and the Israel Science Foundation for support (N.K.).

## References and Notes

- (1) Ulman, A. *An Introduction to Ultrathin Organic Films: From Langmuir-Blodgett to Self-Assembly*; Academic Press: New York, 1991.
- (2) Evans, D. F.; Wennerstrom, H. *The Colloidal Domain*; Wiley: New York, 1999.
- (3) Israelachvili, J. *Intermolecular and Surface Forces*, 2nd ed.; Academic Press: London, UK, 1991.
- (4) Chen, Y. L.; Chen, S.; Frank, C.; Israelachvili, J. *J. Colloid Interface Sci.* **1992**, *153*, 244.
- (5) Fujii, M.; Li, B.; Fukada, K.; Kato, T.; Seimiya, T. *Langmuir* **1999**, *15*, 3689.
- (6) Li, B.; Fujii, M.; Fukada, K.; Kato, T.; Seimiya, T. *J. Colloid Interface Sci.* **1999**, *209*, 25.
- (7) Manne, S.; Gaub, E. H. *Science* **1995**, *270*, 1480.
- (8) Manne, S.; Schaffer, T. E.; Huo, Q.; Hansma, P. K.; Morse, D. E.; Stucky, G. D.; Aksay, I. A. *Langmuir* **1997**, *13*, 6382.
- (9) Atkin, R.; Craig, V.; Biggs, S. *Langmuir* **2001**, *2001*, 6155.
- (10) Atkin, R.; Craig, V.; Wanless, E. J.; Biggs, S. *Adv. Colloid Interface Sci.* **2002**, *266*, 236.
- (11) Atkin, R.; Craig, V.; Wanless, E. J.; Biggs, S. *J. Phys. Chem. B* **2003**, *107*, 2978.
- (12) Ducker, W.; Wanless, E. J. *Langmuir* **1999**, *15*, 160.
- (13) Israelachvili, J.; Pashley, R. *Nature* **1982**, *300*, 341.
- (14) Pashley, R.; McGuiggan, P. M.; Ninham, B.; Fennel Evans, D. *Science* **1984**, *229*, 1088.
- (15) Pashley, R.; Israelachvili, J. *Colloids Surf.* **1981**, *2*, 169.
- (16) Christenson, H.; Claesson, P. M. *Adv. Colloid Interface Sci.* **2001**, *91*, 391.
- (17) Christenson, H.; Claesson, P. M. *Science* **1988**, *239*, 390.
- (18) Claesson, P. M.; Blom, C.; Herder, P.; Ninham, B. *J. Colloid Interface Sci.* **1986**, *114*, 234.
- (19) Raviv, U.; Giasson, S.; Kampf, N.; Gohy, J.-F.; Jerome, R.; Klein, J. *Nature* **2003**, *425*, 163.
- (20) Tsao, Y.-H.; Fennel Evans, D. *Langmuir* **1993**, *9*, 779.
- (21) Eriksson, L. G. T.; Claesson, P. M.; Ohnishi, S.; Hato, M. *Thin Solid Films* **1997**, *300*, 240.
- (22) Ninham, B.; Evans, D. F.; Wel, G. J. *J. Phys. Chem.* **1983**, *87*, 5020.
- (23) Marquies, E. F.; Regev, O.; Khan, A.; Lindman, B. *Adv. Colloid Interface Sci.* **2003**, *100–102*, 83.
- (24) Gravsholt, S. J. *J. Colloid Interface Sci.* **1976**, *57*, 575.
- (25) Nascimento, D. B.; Rapuano, R.; Lessa, M. M.; Carmona-Ribeiro, A. M. *Langmuir* **1998**, *14*, 7387.
- (26) Kang, C.; Khan, A. *J. Colloid Interface Sci.* **1993**, *156*, 218.
- (27) Knock, M. M.; Bain, C. D. *Langmuir* **2000**, *16*, 2857.
- (28) Marra, J. *J. Phys. Chem.* **1986**, *90*, 2145.
- (29) Pashley, R.; McGuiggan, P. M.; Ninham, B.; Brady, J.; Evans, D. F. *J. Phys. Chem.* **1986**, *90*, 1637.
- (30) Menger, F. M.; Littau, C. A. *J. Am. Chem. Soc.* **1993**, *115*, 10083.
- (31) Tabor, D.; Winterton, R. H. S. *Proc. Roy. Soc. A* **1969**, *312*, 435.
- (32) Israelachvili, J.; Adams, G. J. *Chem. Soc., Faraday Trans. I* **1978**, *74*, 975.
- (33) Klein, J. *J. Chem. Soc., Faraday Trans. I* **1983**, *79*, 99.
- (34) Pashley, R.; Israelachvili, J. *J. Colloid Interface Sci.* **1984**, *101*, 511.
- (35) Raviv, U.; Giasson, S.; Frey, J.; Klein, J. *J. Phys.: Condens. Matter* **2002**, *14*, 1.
- (36) Raviv, U.; Perkin, S.; Laurat, P.; Klein, J. *Langmuir* **2004**, *20*, 5322.
- (37) Israelachvili, J.; Pashley, R. *J. Colloid Interface Sci.* **1984**, *98*, 500.
- (38) Parker, J. L.; Claesson, P. M.; Attard, P. *J. Phys. Chem.* **1994**, *98*, 8468.
- (39) Attard, P. *Langmuir* **2000**, *16*, 4455.
- (40) Johnson, K. L.; Kendall, K.; Roberts, A. D. *Proc. Roy. Soc. A* **1971**, *324*, 301.
- (41) Pashley, R. *J. Colloid Interface Sci.* **1980**, *80*, 153.
- (42) These arrangements at the surface have been observed in the past using AFM; however, this is usually under surfactant solution rather than in pure water.